Carbohydrate Polymers 79 (2010) 154–163

Contents lists available at ScienceDirect

Carbohydrate Polymers

journal homepage: www.elsevier.com/locate/carbpol

Effect of sorbitol addition on the physicochemical characteristics of starch–fatty acid systems

Georgia Mantzari, Stylianos N. Raphaelides *, Stylianos Exarhopoulos

Food Process Engineering Laboratory, Department of Food Technology, ATEI of Thessaloniki, P.O. Box 141, Thessaloniki GR-5740, Greece

ARTICLE INFO

Article history:
Received 9 February 2009
Received in revised form 15 July 2009
Accepted 20 July 2009
Available online 25 July 2009

Keywords:
Starch–fatty acid–sorbitol interactions
Starch–sorbitol functionality

ABSTRACT

Aqueous maize starch dispersions (20%) were heated at 100 °C, in the presence of myristic, palmitic or stearic acid potassium salts as well as of sorbitol added at concentrations up to 60% (dry starch). Flow behaviour measurements at 100 °C indicated that interactions took place between the starch–fatty acid systems and sorbitol resulting in viscosity increase which was more pronounced as the sorbitol content increased. Water solubility measurements showed that a major part of sorbitol was easily extracted by excess water whereas sorption experiments revealed that the moisture uptake rate was proportional to sorbitol content of the starch systems examined. Thermomechanical studies indicated that the starch–fatty acid samples containing sorbitol up to 40% exhibited antiplasticizing behaviour. Scanning electron microscopy studies revealed that at sorbitol concentrations over 30%, free sorbitol crystals were formed on the surface of starch–fatty acid samples, whereas the percentage crystallinity as well as the crystallite size of samples were proportional to sorbitol content.

1. Introduction

Starch, the major reserve polysaccharide of plants is being used as a raw material in numerous industrial applications. Apart from being utilized in the food industry as a main ingredient in confectionery, in sauces and in other food commodities it also finds applications in non food uses such as textiles, paper making, packaging etc. Starch is found in nature in the form of granules which are mainly composed of two homopolysaccharides i.e. amylose and amylopectin. Due to its complexity starch exhibits certain unique properties which are not encountered in other polysaccharides and which significantly affect its functionality. These properties are, granule swelling i.e. gelatinization, occurred when starch granules are heated at elevated temperatures in the presence of excess water, retrogradation i.e. crystallization, exhibited by gelatinized starch dispersions upon cooling to ambient temperature and its ability to interact with a number of linear polar and non polar molecules such as fatty acids, fatty alcohols, monoglycerides and others to form inclusion complexes. These phenomena are of paramount importance since they determine the texture of starch systems in solid state (Parker & Ring, 2001). For instance, the starch systems could become rigid and brittle i.e. glassy, loosing their flexibility which is very important either in food items such as bakery products or in products used as packaging materials. To reduce the glass transition temperature of starch systems in order to become more rubbery, normally low molecular weight solutes such as polyols or certain salts or esters are added to starch, since they can act in a way similar to that of plasticizing compounds added to synthetic polymers do (Lourdin, Coignard, Bizot, & Colonna, 1997).

One of these natural plasticizers whose effect on starch vitreous behaviour has been studied, so far, is sorbitol (Lourdin et al., 1997). The research done on the addition of sorbitol to starch systems indicated that not always it behaves as a plasticizer but on the contrary, more often shows an antiplasticizing behaviour depending on its concentration in the starch system (Gaudin, Lourdin, Forssell, & Colonna, 2000; Gaudin, Lourdin, Le Botlan, Ilari, & Colonna, 1999).

Thermally processed starch systems which contained lipids also exhibit a rigid texture due to the formation of crystalline inclusion amylose–lipid complexes which render them difficult to handle and to find uses in various industrial applications.

To the best of our knowledge the effect of sorbitol added to starch–lipid systems as far as their functionality is concerned has not been studied so far. Thus, the aim of the present work was to investigate whether sorbitol could interact with starch–lipid systems and which are the consequences of these probable interactions.

2. Materials and methods

Native maize starch was purchased from Tate & Lylle, Hellas. Its characteristics were moisture content 12.27%, apparent amylose content 21.5 ± 0.6% and total amylose content 26.0 ± 0.3%

* Corresponding author. Tel.: +30 2310 791371; fax: +30 2310 791360.
E-mail address: rafael@food.teithe.gr (S.N. Raphaelides).

0144-8617/$ - see front matter © 2009 Elsevier Ltd. All rights reserved.
doi:10.1016/j.carbpol.2009.07.043

(determined using the method of Morrison & Laignelet, 1983). Fatty acids, myristic, palmitic and stearic (purity 99%) were obtained from Sigma Chemical Company. Sorbitol (purity 98%) was obtained from Carlo Erba. LiCl (>99%), $MgCl_2 \times 6H_2O$ (>99%), K_2CO_3 (>99%), Mg $(NO_3)_2$ (>99%) were purchased from Fluka, NaCl (>99%) obtained from Merck and KNO_3 (>99%) from Riedel-de Haën. All other reagents used were of analytical grade.

2.1. Instrumentation

The preparation of starch–fatty acid–sorbitol systems and the measurement of their flow properties were performed using a custom built pneumatic tube rheometer coded TR-1, designed to perform flow experiments of aqueous systems at elevated temperatures ($\geqslant$100 °C), described in detail elsewhere (Raphaelides & Georgiadis, 2006; Xu & Raphaelides, 1998). Its main features are a thermostatically controlled sample vessel which contains a pin type stirrer and in its bottom is attached a metal tubing through which the sample is passing out to atmosphere. Air pressure is applied to the sample through the top of the hermetically closed vessel. The air pressure is controlled by the controller unit of the instrument. To obtain sample flow curves, a series of mass flow rates of the samples through the tubing were measured in relation to corresponding air pressures applied to the samples. The apparent viscosity η_{app} was calculated from the power law flow equation

$$\eta_{app} = K^* \dot{\gamma}_{corr}^{n-1} \quad (1)$$

where, K is the consistency coefficient (Pa $*$ s^n), $\dot{\gamma}_{corr}$ is the corrected shear rate and n is the flow behaviour index (van Wazer, 1963).

The validity of the viscometer was verified by measuring the viscosity of a standard silicon fluid (Brookfield Engineering Laboratories, Inc.) at 25 °C.

2.2. Sample preparation

Three series of experiments were carried out as follows: In the first series, aqueous starch dispersion (starch content 20% w/w) was heated inside the sample vessel (capacity 70 ml) of TR-1 from ambient temperature to 100 °C, under continuous stirring at 50 rpm rotational speed. In the second series, fatty acid potassium salt aqueous solution was added to the starch dispersion at ambient temperature before the start of heating. The fatty acid concentration employed exceeded by ~5% the concentration known to be necessary to interact with the total amount of available (apparent) amylose present in the sample to form fully saturated, with fatty acid anions, amylose helices (Karkalas & Raphaelides, 1986). Then, the sample was heated to 100 °C under continuous stirring (50 rpm). Both series of samples were designated as the control ones. In the third series sorbitol was added to starch dispersions with or without the addition of fatty acid K salts. Sorbitol, in powder form, was added together with starch in the rheometer's sample vessel followed by the addition of the appropriate amount of water together with or without the addition of fatty acid soap aqueous solution. Then, the mixture was heated from ambient temperature to 100 °C under continuous stirring (50 rpm). The composition of all samples prepared and examined in this work is shown in Table 1.

2.3. Viscosity measurements

All samples prior to their viscosity measurements were kept for 30 min under continuous stirring (50 rpm) at 100 °C for starch gelatinization and possible starch interactions with the other components, present in the sample, to be completed. The tubing fixed at the bottom of the rheometer's sample vessel through which the samples were passing out to atmosphere had a length of 52 mm and an internal diameter of 2.16 mm. Samples contained stearic acid and 40% or 60% sorbitol, could not be measured since they were solidified as soon as they were coming out of the measuring unit of the TR-1 to ambient temperature.

Quantities of all samples prepared and measured using the TR-1 were collected for further examination and stored at ambient temperature for one week prior to their examination in order their moisture content to be equilibrated.

2.4. Moisture content

It was gravimetrically determined by heating the samples at 130 °C till constant weight.

2.5. Water solubility index (WSI)

WSI, defined as the water soluble fraction of the sample expressed as percentage of dry sample and being a measure of the dispersibility of the material was measured by the method of Anderson, Conway, Pfeifer, and Griffin (1969).

2.6. Adsorption isotherms

Samples were dried in a vacuum oven at 50 °C for at least 48 h, till constant weight. Quantities (~0.5 g) of the dried samples, contained in preweighed polypropylene dishes, were weighed in an analytical balance and placed over saturated (at 40 °C) salt solutions of known relative humidity values in hermetically sealed glass containers (capacity 800 mL). Then, the containers were stored in a thermostatically controlled chamber at 30 °C. The dishes were weighed, at regular time intervals, till constant weight. It was found that equilibrium was achieved after a week. The adsorption experiments were replicated three times. The adsorption isotherms were drawn using as coordinates the parameters, percentage relative humidity and water content i.e. the weight difference of the sample at the beginning of the storage period at a certain relative humidity environment and after the equilibrium in this environment was achieved, over the initial weight of the dried sample.

Table 1
Plot of samples examined.

Sorbitol content (dry starch basis) (%)	Sample[a]			
0 (Control)	Starch–water	Starch–water–myristic acid	Starch–water–palmitic acid	Starch–water–stearic acid
10	Starch–water	Starch–water–myristic acid	Starch–water–palmitic acid	Starch–water–stearic acid
20	Starch–water	Starch–water–myristic acid	Starch–water–palmitic acid	Starch–water–stearic acid
30	Starch–water	Starch–water–myristic acid	Starch–water–palmitic acid	Starch–water–stearic acid
40	Starch–water	Starch–water–myristic acid	Starch–water–palmitic acid	Starch–water–stearic acid
60	Starch–water	Starch–water–myristic acid	Starch–water–palmitic acid	Starch–water–stearic acid

[a] Fatty acids were added in the form of aqueous potassium salt solutions.

2.7. Modulus of elasticity and rheological glass transition temperature

Samples formulated into strips of dimensions 36 × 10 × 3 mm were measured in a DMA rheometer Bohlin CVOR 150 (Bohlin Ltd., UK), operated at the oscillatory mode under constant frequency 0.1 Hz, constant stress 150 Pa and programmed heating rate of 5 °C/min. The strain in all samples examined ranged from 10×10^{-7} to 10×10^{-5} which was well within the linear viscoelastic region. The parameters measured were the storage modulus G′ and tan δ in relation to the temperature of heating.

2.8. X-ray diffraction

Samples were immersed in liquid nitrogen and immediately were pulverized by means of a pestle and a mortar. The powder obtained was passed through a sieve with an aperture of 800 μm. The

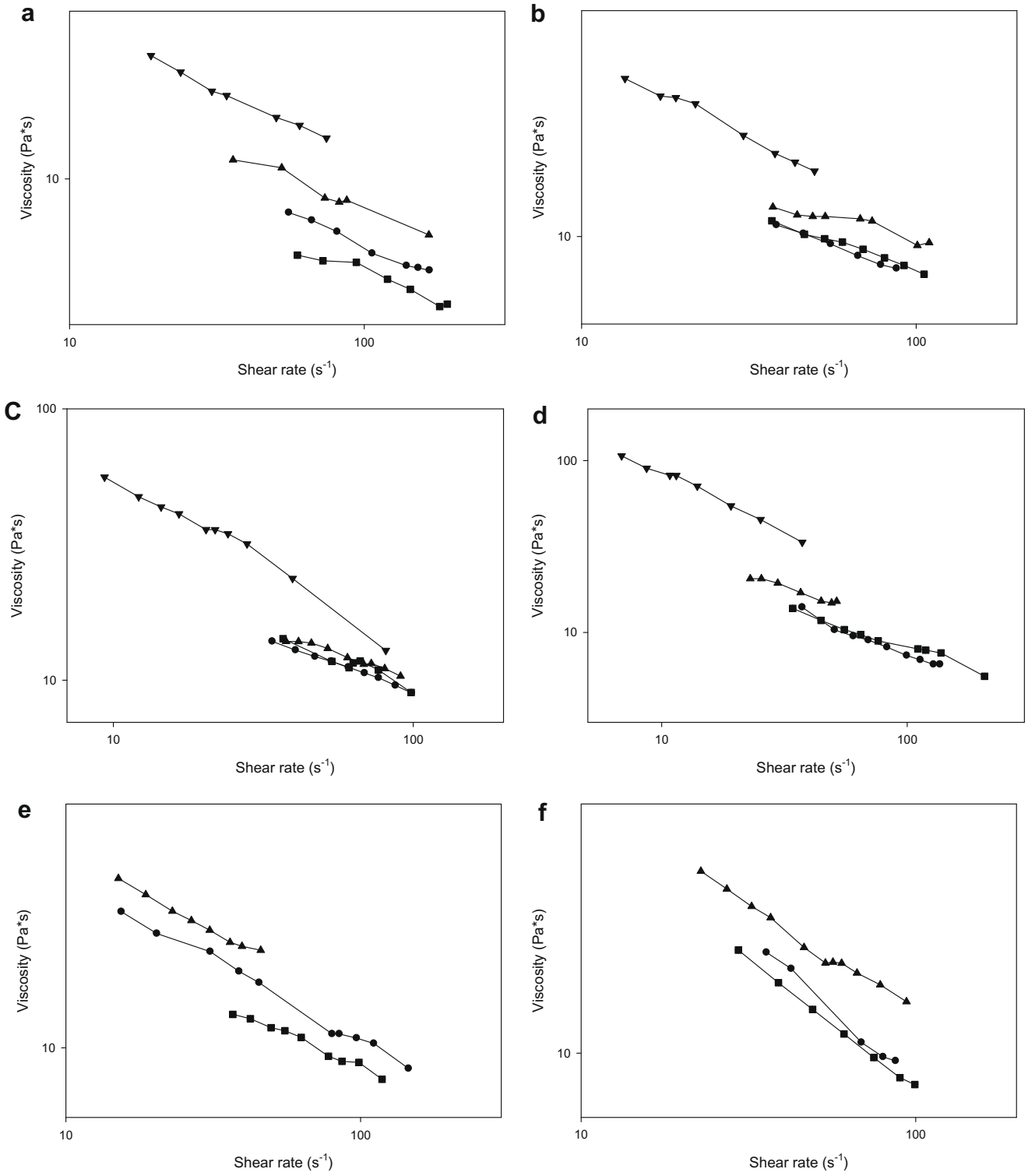

Fig. 1. Flow curves of starch–fatty acid systems with or without added sorbitol at 100 °C. Symbols denote: ●, starch (no fatty acid); ■, starch–myristate; ▲, starch–palmitate; ▼, starch–stearate. Letters denote sorbitol content (dry starch): a, no sorbitol added; b, 10%; c, 20%; d, 30%; e, 40%; f, 60%.

samples were examined using a PANalytical X'Pert Pro diffractometer (Panalytical, Netherlands) with a Cu Ka_1 radiation (λ = 1.5405980 Å). The diffractometer was operated in reflection mode at 45 kV and 40 mA. A divergence slit of 1°, an antiscatter slit of 2° and a receiving slit of 0.4 mm were used. Measurements were taken between 6° and 35° (2θ) with a step size of 0.04° and a scan speed of 0.008°/s.

For the determination of the relative crystallinity the data were normalized from 9° to 30° (2θ) and the background was determined using the X'Pert HighScore PANalytical software. The crystallinity index (X_c) was calculated according to the following equation (Stribeck, 2007):

$$X_c = \frac{I_{cr}}{I_{am} + I_{cr}} \quad (2)$$

where, I_{cr} is the integrated area between the crystalline reflections and the amorphous halo and I_{am} the integrated area between the amorphous halo and the baseline.

Crystallite size was determined according to Scherrer's formula (Brundle, Evans, & Wilson, 1992):

$$L \approx \frac{\lambda}{\mathrm{FWHM} \times \cos\theta} \quad (3)$$

where, L is the crystallite size in Å, λ the wavelength and FWHM the Full Width at Half-Maximum.

2.9. Scanning electron microscopy

Samples were mounted on aluminum stubs with sticky double-side carbon tape. No special treatment applied to the specimens and no coating was needed. Examination was performed by a Carl Zeiss EVO 50 VP scanning electron microscope (Carl Zeiss SMT, Ltd., UK) at 5 kV accelerating voltage, under variable pressure mode, suitable for non-conductive specimens, at pressure of 30 Pa. A Variable Pressure Secondary Electron (VPSE) detector was used.

3. Results and discussion

3.1. Flow behaviour of starch–fatty acid–sorbitol systems

Fig. 1a shows flow curves of maize starch (20%)–fatty acid systems heated at 100 °C without added sorbitol. It can be seen that the addition of fatty acid to starch dispersion significantly affected its viscosity. Thus, the addition of myristic acid caused the reduction of viscosity of the starch system whereas palmitic acid slightly increased the viscosity and the presence of stearic acid considerably increased it. Similar results were reported for maize starch (10%)–fatty acid systems heated at 98 °C (Raphaelides & Georgiadis, 2006). At 100 °C all starch granules have been destroyed due to swelling and to continuous stirring as light microscopy observations revealed (data not shown). Thus, the amylose present in the granules is readily available to interact with the fatty acids to form inclusion helical complexes. Amylose molecules, in solution, assume the random coil conformation whereas when they are complexed with fatty acid anions assume the conformation of extended helices (Karkalas & Raphaelides, 1986). The viscosity decrease because of the presence of myristate anions could be attributed to the existence of many kinks formed along the amylose chain due to the presence of guest molecules with rather short chain length such as the myristate ions. Thus, the amylose helices are flexible and deformable and this affects the viscosity exhibited by the starch–myristate system in comparison to that of the starch system without the presence of myristate ions. On the other hand, when palmitate or stearate ions were added to the starch system then the complexed amylose helices became more rigid due to the existence of fewer kinks than in the case of myristate ions and the viscosity of the starch system increased proportionally to the chain length of the fatty acid added. Moreover, the rigidity exhibited by the amylose helices contained stearate ions might have helped to link together adjacent amylose chains through hydrogen bonding thus increasing the hydrodynamic volume of the macromolecules with the result the viscosity increase of the starch–stearate system. Similar results were reported concerning the flow behaviour of potato starch–fatty acid systems in alkaline solution (Raphaelides, 1992). Moreover, it is known (Banks & Greenwood, 1971; Godet, Tran, Delage, & Buleon, 1993) that the amylose helical cavity is hydrophobic in order to accommodate the lipid monomers whereas at the outside surface of the helix active hydroxyls are exposed together with the carboxyl groups of the fatty acid molecules, which, it has been reported (Buleon, Colonna, Planchot, & Ball, 1998; Carlson, Larsson, Dinh-Nguyen, & Krog, 1979; Godet et al., 1993; Snape, Morrison, Maroto-Valer, Karkalas, & Pethrick, 1998), are located outside the helical cavity due to steric hindrance. These active groups could form links between adjacent amylose helices. This assumption is supported by the increased pseudoplasticity of the starch–stearate system in comparison to the other starch–fatty acid systems since the flow behaviour index of the starch–stearate system was significantly lower than those of the other starch systems (Table 2). That means, at high shear rates dissociation of these links between the adjacent macromolecules occurred and the viscosity of the starch–stearate system was rapidly reduced.

When sorbitol was added to starch–fatty acid systems then their viscosity was increased (Fig. 1b–f). In fact, the increase in viscosity of all samples examined was proportional to the sorbitol content increase. Moreover, it is observed that starch–myristate systems in which sorbitol was added exhibited similar viscosity to that of the analogous starch–sorbitol systems (control). It is noteworthy, that when sorbitol was added to starch–stearate systems in quantities from 40% to 60% of dry starch then the samples were immediately gelled inside the sample holder of the rheometer operating at 100 °C and it was extremely difficult to pass through the exit tubing even by applying air pressure of 2 bars on the sample. The results indicated that sorbitol interacts with the starch system especially when amylose acquires the V-structure i.e. being complexed with fatty acids. This could be attributed

Table 2
Flow behaviour index (n) of starch–fatty acid systems with and without the addition of sorbitol.[a]

Samples	Flow behaviour index (n)
Starch–water	0.539
Starch–water–myristic acid	0.620
Starch–water–palmitic acid	0.680
Starch–water–stearic acid	0.476
Starch–water–10% sorbitol	0.566
Starch–water–myristic acid–10% sorbitol	0.612
Starch–water–palmitic acid–10% sorbitol	0.696
Starch–water–stearic acid–10% sorbitol	0.416
Starch–water–20% sorbitol	0.602
Starch–water–myristic acid–20% sorbitol	0.645
Starch–water–palmitic acid–20% sorbitol	0.647
Starch–water–stearic acid–20% sorbitol	0.340
Starch–water–30% sorbitol	0.481
Starch–water–myristic acid–30% sorbitol	0.545
Starch–water–palmitic acid–30% sorbitol	0.486
Starch–water–stearic acid–30% sorbitol	0.315
Starch–water–40% sorbitol	0.415
Starch–water–myristic acid–40% sorbitol	0.587
Starch–water–palmitic acid–40% sorbitol	0.447
Starch–water–60% sorbitol	0.314
Starch–water–myristic acid–60% sorbitol	0.370
Starch–water–palmitic acid–60% sorbitol	0.480

[a] Sorbitol content as percentage of dry starch content.

to the fact that the external surface of the amylose helices bears hydroxyl groups which could interact with the hydroxyl groups of sorbitol to form hydrogen bridges. Thus, the hydrodynamic volume of amylose molecules increased resulting in the viscosity increase. As for the case of starch–stearate system the considerable increase in viscosity might not only be attributed to amylose–sorbitol interactions but also to amylose–amylose interactions which could form entanglements thanks to enhanced rigidity of amylose–stearate helices. The assumption of entanglement formation could explain the greater pseudoplasticity exhibited by the starch–stearate–sorbitol systems in comparison to the other starch systems (Table 2). Thus, as the shear rate increased the viscosity dramatically decreased possibly due to disentanglement which allowed the amylose molecules to move separately one from the other. The instantaneous gelation of starch–stearate samples containing 40% or 60% sorbitol could be attributed to the formation of permanent cross links due to these entanglements. On the other hand, it can be seen (Fig. 1e and f) that the viscosity exhibited by the starch systems with or without fatty acid containing 60% sorbitol is the same with that exhibited by the analogous samples containing 40% sorbitol. This is an indication that at 40% sorbitol content all the available hydroxyl groups of sorbitol molecules have interacted with all the available hydroxyl groups of amylose thus further addition of sorbitol molecules did not necessarily lead to further interaction with amylose molecules.

3.2. Moisture content

Fig. 2 shows the residual moisture content of starch–fatty acid samples with or without added sorbitol. All samples without sorbitol had higher moisture content than those contained sorbitol. It is noteworthy that samples contained sorbitol up to 40% showed a gradual decrease in their moisture content whereas samples contained 60% sorbitol showed a slight increase in their moisture content. Similar results were reported by Lourdin et al., 1997; Gaudin et al., 1999). Moreover, starch samples without fatty acids had higher moisture content in most cases than the analogous samples containing fatty acids. This could be attributed to the different crystalline structure which acquires the uncomplexed amylose during retrogradation which is that of B-type double left handed helix in relation to that exhibited by the amylose–fatty acid complexes which is that of V-structure. It is well known (Belitz, Grosch, & Schieberle, 2004) that B-structure has the ability to hold water molecules between helices in contrast to V-structure which is more compact and does not contain water between adjacent helices. The reduction of moisture content in samples containing sorbitol could be attributed to the presence of sorbitol molecules in space normally occupied by water molecules. As for the slight increase in moisture content in samples containing 60% sorbitol, this might be due to binding of water molecules by free (not bound to starch) sorbitol molecules, since sorbitol is hygroscopic.

3.3. Water solubility index (WSI)

Fig. 3 shows the WSI results of starch–fatty acid samples with or without added sorbitol. It can be seen that there is a significant increase of solubilized material proportional to sorbitol content of

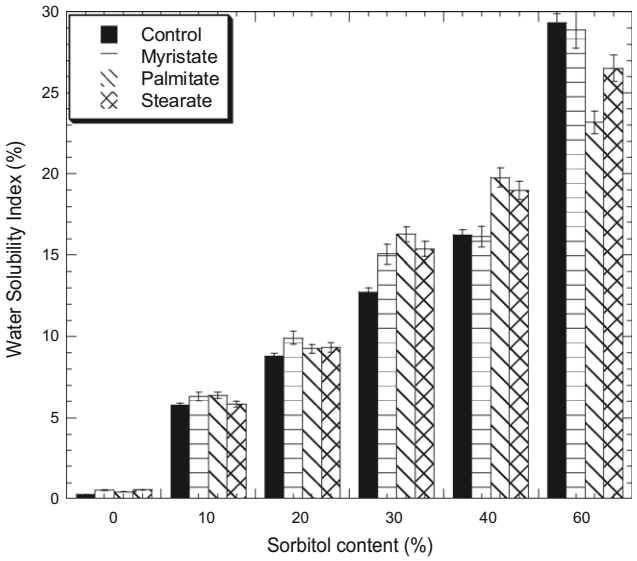

Fig. 3. Water solubility index of starch–fatty acid–sorbitol systems as a function of sorbitol content (% dry starch).

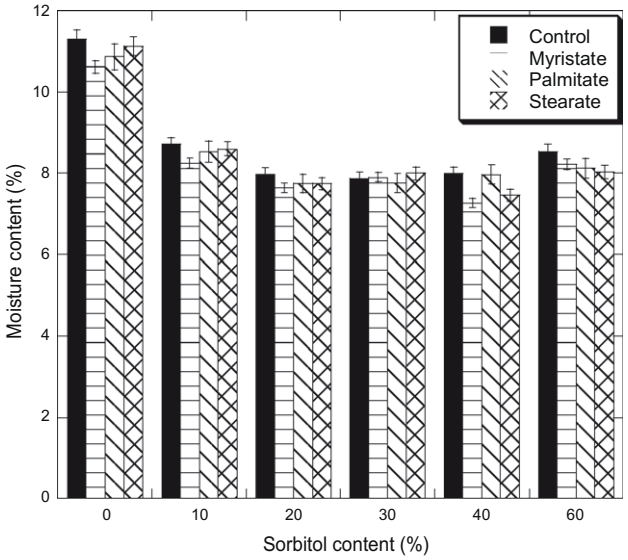

Fig. 2. Residual moisture content of starch–fatty acid–sorbitol systems as a function of sorbitol content (% dry starch).

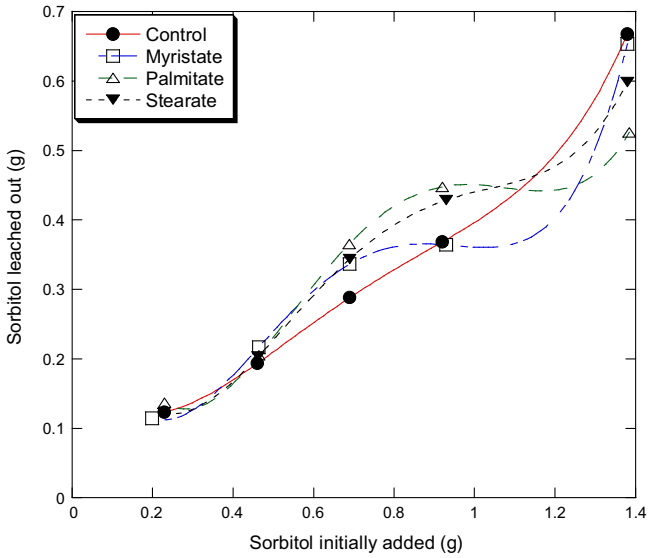

Fig. 4. Sorbitol leached out of starch–fatty acid–sorbitol systems as a function of the initially added sorbitol to the starch systems.

the samples. The solubilized material must be almost entirely sorbitol which has much greater affinity to water than to amylose, hence it easily migrates to water when it comes in contact with that. Fig. 4 shows the residual sorbitol content of samples after leaching with water as a function of sorbitol content initially added to samples during their preparation. The difference in shape between the curve of the control (exponential) and the curves of samples with fatty acids (sigmoid) shows that the amylose crystalline

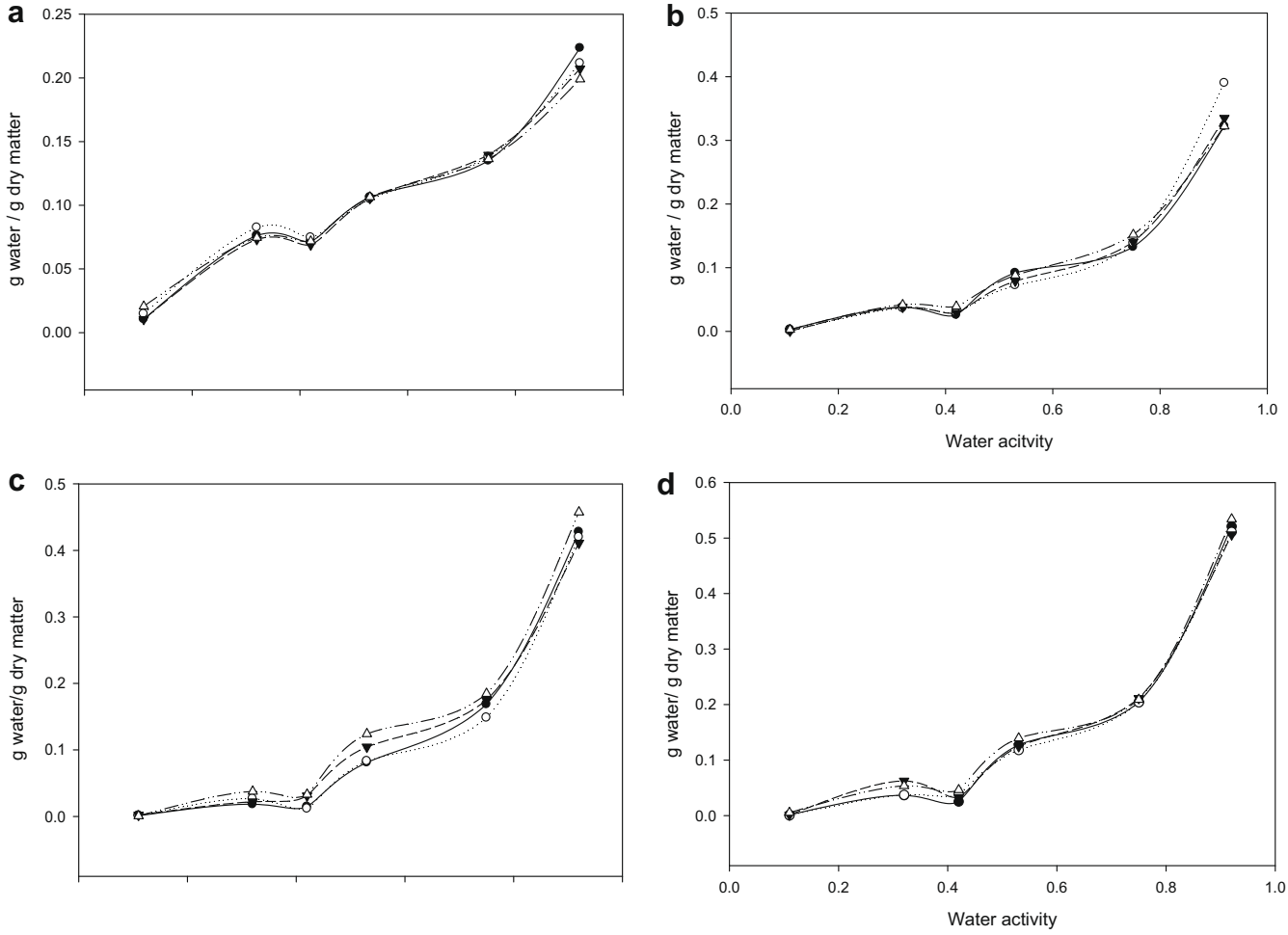

Fig. 5. Sorption isotherms of starch–fatty acid systems with or without added sorbitol at 30 °C. Symbols denote: ●, starch (no fatty acid); ○, starch–myristate; ▼, starch–palmitate; Δ, starch–stearate. Letters denote sorbitol content (dry starch): a, no sorbitol added; b, 20%; c, 40%; d, 60%.

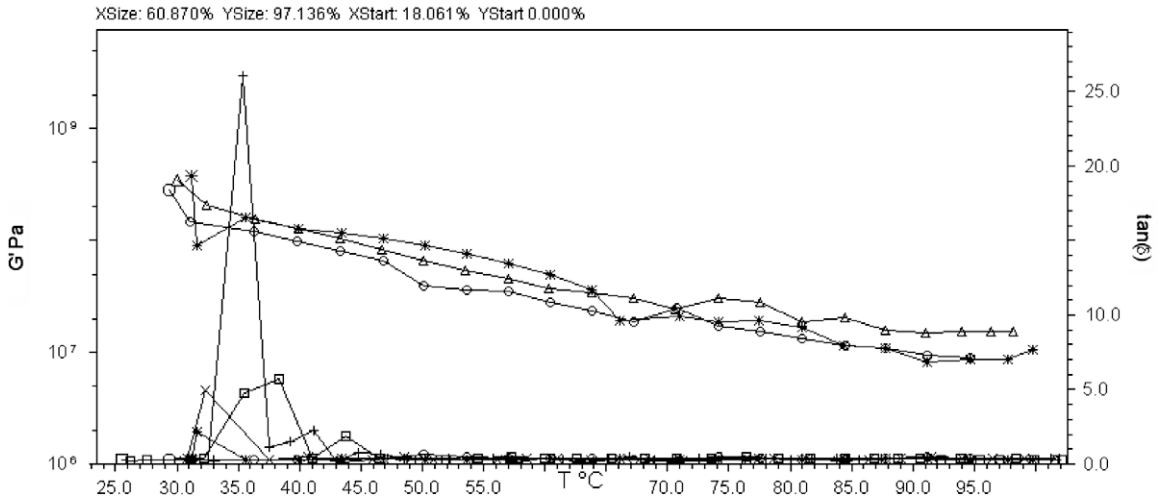

Fig. 6. Storage modulus (G′) and tan δ of starch–fatty acid systems with 60% added sorbitol as a function of heating temperature. Symbols denote G′, tan δ: Δ, +, control (no fatty acid added); O, x, starch–myristate system; ∗, □, starch–palmitate system.

structure, in any case, plays a significant role in the amount of sorbitol leached out. The abrupt increase of the amount of sorbitol leached out, when 60% of sorbitol was added to starch system should be attributed to the fact that a substantial part of sorbitol was mechanically trapped between the amylose helices as it has been shown in the microphotographs taken by *SEM* (Fig. 7). This happened possibly due to complete interaction of the available hydroxyl groups of amylose molecules with sorbitol molecules, thus the remaining excess sorbitol could easily leach out when it came in contact with excess water.

3.4. Sorption isotherms

Fig. 5 shows the sorption isotherms of starch–fatty acid samples with or without added sorbitol. It can be seen that all samples showed similar behaviour as far as water vapour adsorption is concerned. Besides, the addition of sorbitol caused a significant increase in moisture uptake which was proportional to sorbitol content and the relative humidity. That is, the higher the relative humidity and the sorbitol content were the higher the amount of water being adsorbed. Lourdin et al. (1997) reported similar results for potato starch–sorbitol systems. The shape of the isotherms is rather peculiar and none of the sorption isotherm models reported in literature such as BET or GAB could fit. However, this was not due to the presence of sorbitol since the shape of sorbitol isotherm is different, typical that of sugars (data not shown). The cause of this behaviour might be the crystallization of starch components either due to starch retrogradation or due to amylose–fatty acid complex formation. Bizot (1983) emphasized that for starch the GAB model does not fit when it becomes more crystalline at water activities from 0.6 to 0.7.

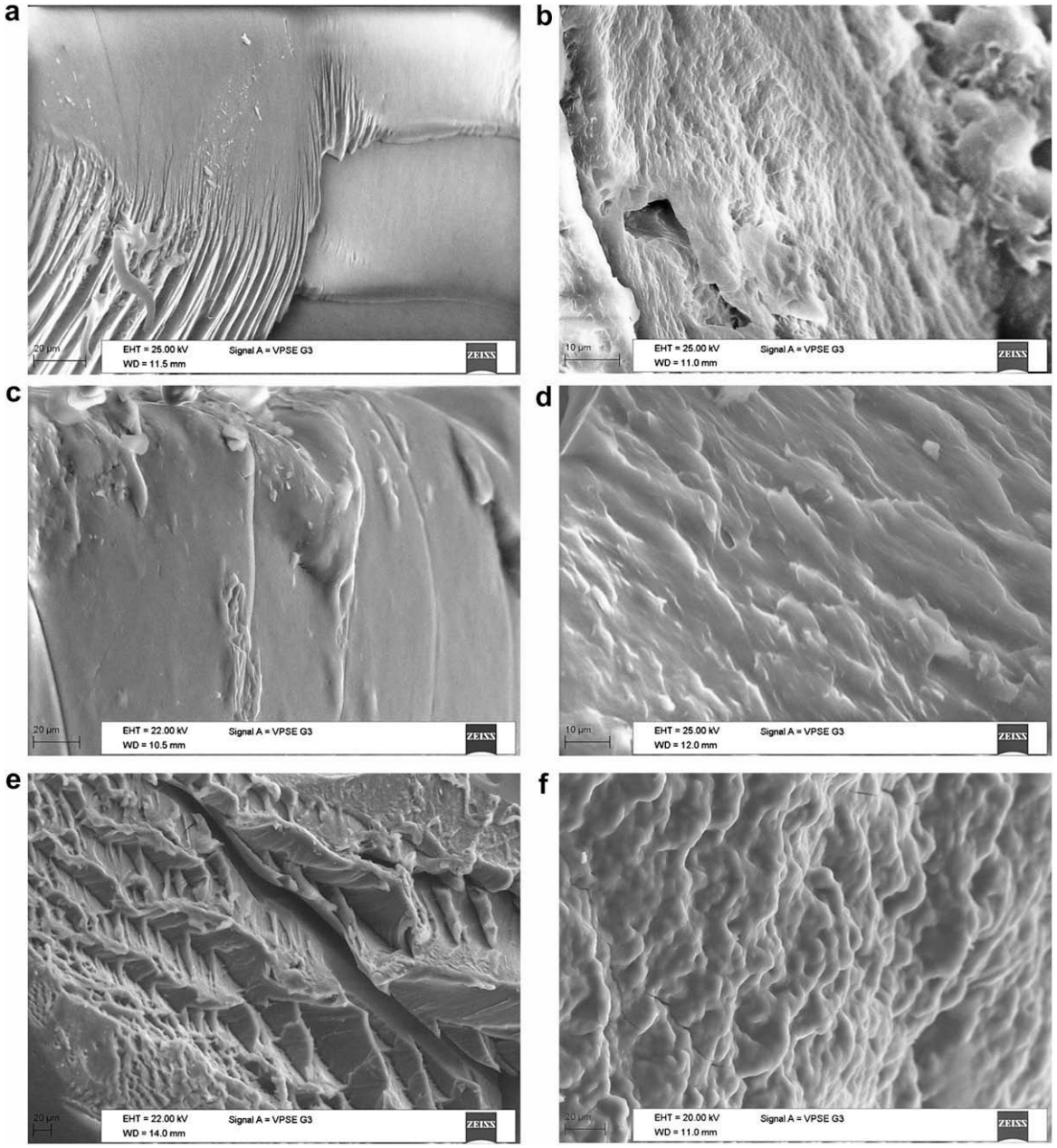

Fig. 7. Microphotographs of starch–fatty acid systems with or without added sorbitol. Letters denote: a, starch; b, starch–stearate; c, starch–10% sorbitol; d, starch–stearate–10% sorbitol; e, starch–myristate–20% sorbitol; f, starch–stearate–20% sorbitol; g, starch–30% sorbitol; h, starch–myristate–30% sorbitol; i, starch–palmitate–30% sorbitol; j, starch–stearate–30% sorbitol; k, starch–40% sorbitol; l, starch–myristate–40% sorbitol; m, starch–stearate–40% sorbitol.

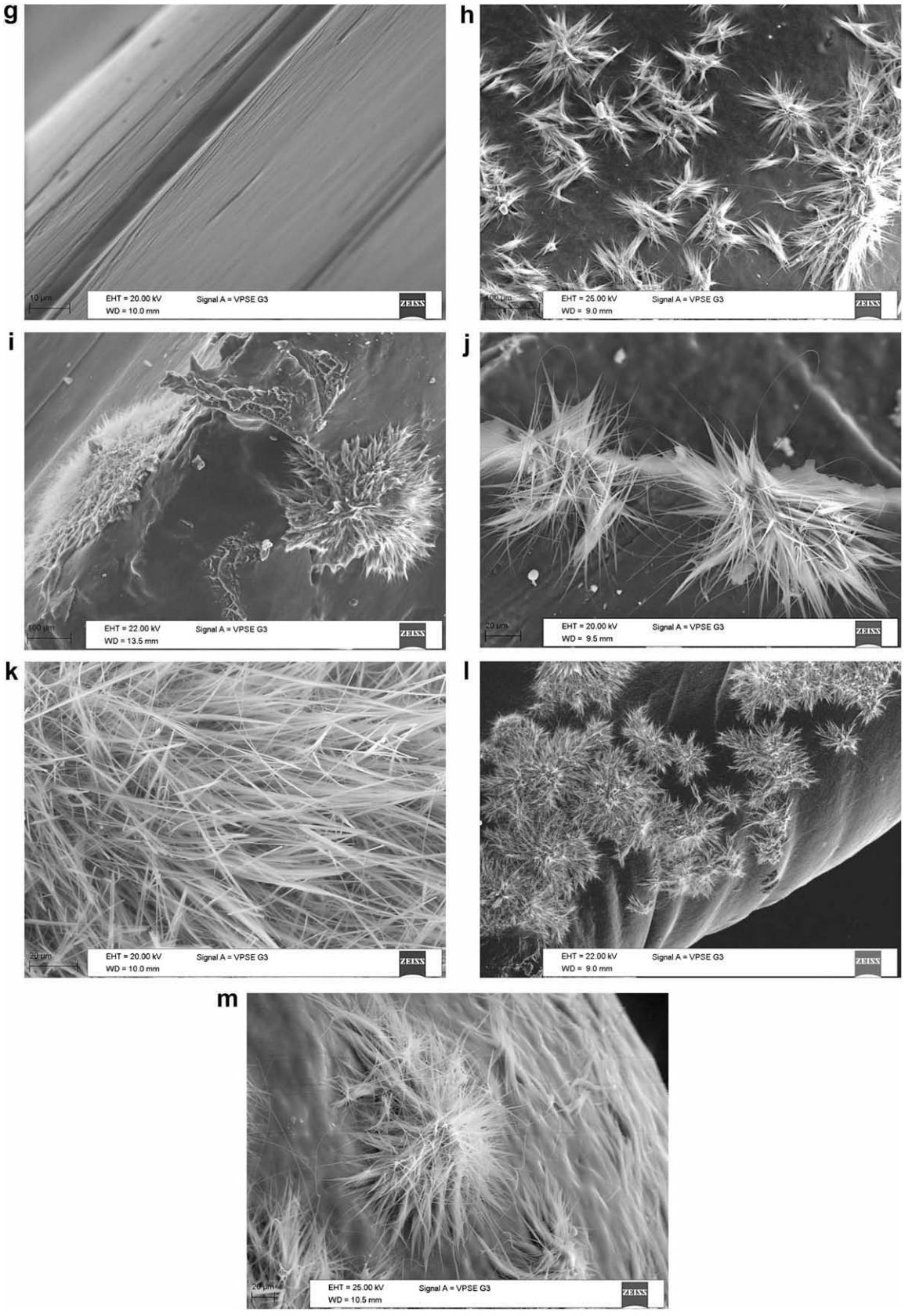

Fig. 7 (*continued*)

3.5. Thermomechanical behaviour

Fig. 6, shows storage modulus (G′) and tan δ curves as a function of temperature of heating of starch–fatty acid systems with 60% sorbitol content.

Samples contained sorbitol up to 40% could not be measured since they were too rigid and brittle to be fixed, intact, in the measuring unit of the rheometer. The only samples which, it was possible to measure were those with 60% sorbitol since they were a little more flexible than the others. The rheological glass transition temperatures (T_g) measured from the tan δ peaks for the three samples examined were approximately 35 °C for the control, 32 °C for the starch–myristate and 38 °C for the starch–palmitate samples. It can be seen that the sample with palmitic was slightly more rigid than the control and the control slightly more rigid than the sample with myristic acid. Gaudin et al. (1999), found that sorbitol concentrations up to 27% (dry starch) caused an antiplasticizing effect to potato starch samples by rendering them rigid and brittle whereas over this value (27%) the starch samples became rubbery and exhibited the behaviour of a plasticized polymer. According to their findings, thermomechanical T_g was decreased from 70 °C at 9.4% sorbitol content (dry starch) to 40 °C for 36% sorbitol content.

3.6. Scanning electron microscopy

Fig. 7 shows microphotographs of starch–fatty acid systems with or without added sorbitol. It can be seen that the control samples i.e. starch (a), starch–myristate and starch–stearate (b) show a continuous phase without any trace of starch granules. The main difference is that the starch and starch–myristate samples show a similar smooth appearance whereas the starch–stearate sample shows a rough surface probably due to the existence of amylose helices embedded in an amylopectin matrix. The addition of 10% sorbitol did not change much the appearance of starch sample (c) whereas the starch–myristate sample showed some grooves which in the case of starch–stearate sample (d) became many and very apparent. The addition of 20% sorbitol did not affect much the appearance of starch sample, however, in the case of starch–myristate (f) and starch–stearate (g) caused a spectacular change in the appearance of both samples showing a very irregular surface with many grooves. The concentration increase to 30% of sorbitol added to starch sample did not cause any noticeable change in the appearance of the sample's surface whereas in all starch–fatty acid samples (h–j) caused the appearance of sorbitol crystals on the sample's surface.

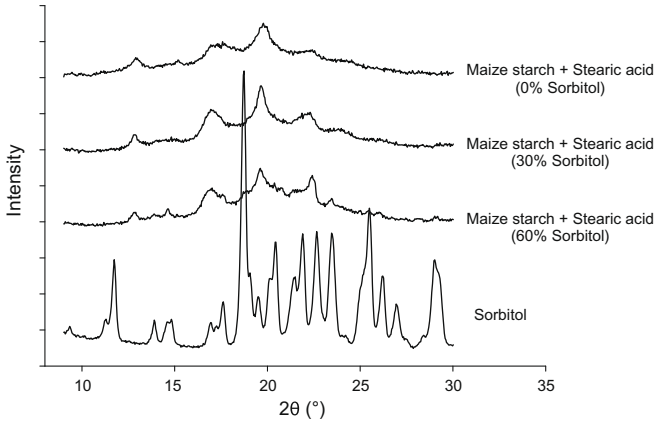

Fig. 8. X-ray diffraction patterns of crystalline pure sorbitol and starch–stearate systems with and without added sorbitol.

It seems that at 30% concentration sorbitol is already in excess to be totally accommodated or occluded between the amylose helices thus whatever amount was left free it formed crystals on the surface of the samples. Further increase of sorbitol addition (40%) to starch samples caused the appearance of crystals to all samples regardless of whether they contained fatty acid or not (k–m). The same phenomenon was observed in starch samples contained 60% sorbitol. There seems to be a notable difference between the appearance of sorbitol crystals on the surface of starch samples and those on the surface of starch–fatty acid samples. That is, in starch samples the sorbitol crystals having the shape of needles literally covered the sample's surface haphazardly whereas, in the case of starch–fatty acid samples excess sorbitol formed clusters of needle like crystals on the sample's surface.

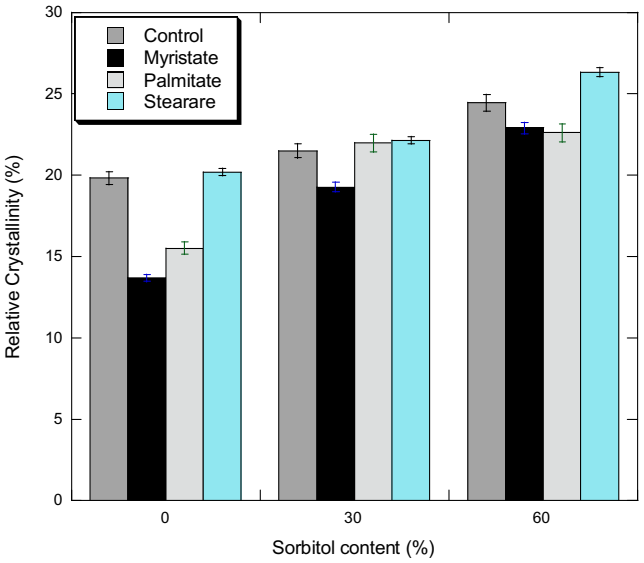

Fig. 9. Relative crystallinity of starch–fatty acid–sorbitol systems as a function of sorbitol content (dry starch).

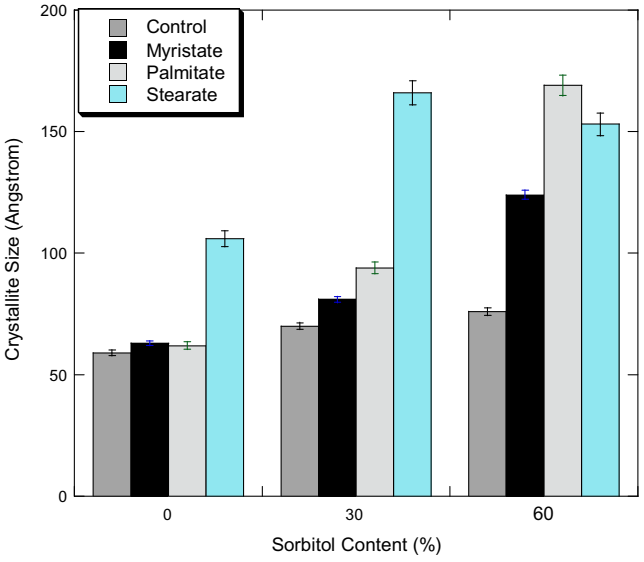

Fig. 10. Crystallite size of starch–fatty acid–sorbitol systems as a function of sorbitol content (dry starch).

3.7. X-ray analysis

Fig. 8 shows the effect of the addition of sorbitol on the diffraction pattern of starch–stearate system. Without sorbitol the system exhibits the well known V-pattern which with the addition of sorbitol became even more pronounced especially at high sorbitol content (60%). It is noteworthy that although sorbitol was previously shown (*SEM* microphotographs) to be present to the system partly in a free state, this is not revealed by X-ray analysis. Fig. 8 shows the characteristic pattern of crystalline pure sorbitol, which differs from that of starch–stearate–sorbitol systems which as it was already mentioned, exhibit the characteristic V-pattern of amylose–fatty acid complexes. That possibly means the amylose–fatty acid complexes comprise the majority of the crystalline structure and they can effectively mask the effect of free sorbitol's presence. However, determination of relative crystallinity of samples revealed that the addition of sorbitol significantly increased the crystallinity of starch–fatty acid systems (Fig. 9). Moreover, the crystallite size of starch–fatty acid systems was significantly increased due to the addition of sorbitol to starch samples (Fig. 10).

4. Conclusions

The present study showed that sorbitol addition to starch–fatty acids systems did cause changes in their physicochemical characteristics which are

- Sorbitol interacts with the hydroxyl groups of thermoplastic starch molecules regardless if they are complexed with lipids or not. However, these interactions are not strong enough to prevent migration of sorbitol molecules to water when they come into contact with excess of water.
- Sorbitol causes a strong antiplasticizing effect to thermoplastic starch systems at least at concentrations up to 40% (dry starch).
- Moisture uptake by starch–fatty acid systems is greatly enhanced in the presence of sorbitol and the adsorption rate is proportional to sorbitol content of starch systems.
- Free sorbitol forms crystals in starch–fatty acid systems when its concentration in the systems exceeds 30% (dry starch).
- The relative crystallinity of starch–fatty acid systems increases when sorbitol added to them.
- Crystal size of starch–fatty acid systems greatly increases depending on the sorbitol concentration added to them.

References

Anderson, R. A., Conway, H. F., Pfeifer, V. F., & Griffin, L. E. J. (1969). Gelatinization of corn grits by roll- and extrusion cooking. *Cereal Science Today, 14*(4–7), 11–12.

Banks, W., & Greenwood, C. T. (1971). The conformation of amylose in dilute solution. *Starch/Staerke, 23*, 300–314.

Belitz, H. D., Grosch, W., & Schieberle, P. (2004). *Food chemistry* (3rd ed.). Heidelberg: Springer Verlag.

Bizot, H. (1983). Using the "G.A.B." model to construct sorption isotherms. In R. Jowitt, F. Escher, B. Hallström, H. F. T. Meffert, W. E. L. Spiess, & G. Vos (Eds.), *Physical properties of foods* (pp. 43–54). London: Applied Science Publishers.

Brundle, R. C., Evans, C. A., & Wilson, S. (1992). *Encyclopedia of materials characterization-surfaces, interfaces, thin films*. Boston: Butterworth-Heinemann.

Buleon, A., Colonna, P., Planchot, V., & Ball, S. (1998). Starch granules: structure and biosynthesis. Mini Review. *International Journal of Biological Macromolecules, 23*(8), 5–112.

Carlson, T. L.-G., Larsson, K., Dinh-Nguyen, N., & Krog, N. (1979). A study of the amylose–monoglyceride complex by Raman spectroscopy. *Starch/Staerke, 31*, 222–224.

Gaudin, S., Lourdin, D., Forssell, P. M., & Colonna, P. (2000). Antiplasticisation and oxygen permeability of starch–sorbitol films. *Carbohydrate Polymers, 43*, 33–37.

Gaudin, S., Lourdin, D., Le Botlan, D., Ilari, J. L., & Colonna, P. (1999). Plasticisation and mobility in starch–sorbitol films. *Journal of Cereal Science, 29*, 273–284.

Godet, M. C., Tran, V., Delage, M. M., & Buleon, A. (1993). Molecular modelling of the specific interactions involved in the amylose complexation by fatty acids. *International Journal of Biological Macromolecules, 15*, 11–16.

Karkalas, J., & Raphaelides, S. (1986). Quantitative aspects of amylose–lipid interactions. *Carbohydrate Research, 157*, 215–234.

Lourdin, D., Coignard, L., Bizot, H., & Colonna, P. (1997). Glass transition temperature versus equilibrium relative humidity. *Polymer, 38*, 5401–5406.

Morrison, W. R., & Laignelet, B. (1983). An improved colorimetric procedure for determining apparent and total amylose in cereal and other starches. *Journal of Cereal Science, 1*, 9–20.

Parker, R., & Ring, S. G. (2001). Aspects of the physical chemistry of starch. *Journal of Cereal Science, 34*, 1–17.

Raphaelides, S. N. (1992). Flow behaviour of starch–fatty acid systems in solution. *Lebensmittel Wissenschaft und Technologie, 25*, 95–101.

Raphaelides, S. N., & Georgiadis, N. (2006). Effect of fatty acids on the rheological behaviour of maize starch dispersions during heating. *Carbohydrate Polymers, 65*, 81–92.

Snape, C. E., Morrison, W. R., Maroto-Valer, M. M., Karkalas, J., & Pethrick, R. A. (1998). Solid state ^{13}C NMR investigation of lipid ligands in V-amylose inclusion complexes. *Carbohydrate Polymers, 36*, 225–237.

Stribeck, N. (2007). *X-ray scattering of soft matter*. Berlin: Springer.

van Wazer, J. R. (1963). *Viscosity and flow measurements: A laboratory handbook of rheology*. New York: Interscience.

Xu, Z.-M., & Raphaelides, S. N. (1998). Flow behavior of concentrated starch dispersions using a tube rheometer of novel design. *Journal of Texture Studies, 29*, 1–13.